ORIGINAL ARTICLE

Shigeru Yamauchi · Shuichi Doi

Raman spectroscopic study on the behavior of boric acid in wood

Abstract Raman spectra of Japanese cedar (*Cryptomeria japonica* D. Don) treated by vacuum impregnation with aqueous boric acid solutions (8.1×10^{-2} to $7.29 \times 10^{-1}\,mol\,dm^{-3}$) were recorded using a near-infrared laser as an excitation source. Raman spectroscopic measurements were carried out on treated wood blocks of two sizes: 20(T) $\times$ 20(R) $\times$ 5(L) mm (A-type) and 15(T) $\times$ 15(R) $\times$ 50(L) mm (B-type). Our attention was focused on a prominent band (ν_1) assigned to a symmetrical stretching vibration of the BO_3 group because no Raman band due to boron species was observed except bands of $B(OH)_3$. We observed a change in ν_1 band intensity with increasing boric acid concentration in the aqueous solution used to treat the A-type wood blocks and investigated the correlation between the intensity and the peak-top wavenumber. Raman line maps in the longitudinal direction of the treated B-type wood blocks revealed that $B(OH)_3$ is concentrated near the cut ends. These results suggested that two groups of $B(OH)_3$ exist in wood in terms of the chemical species in the nearest neighbor sphere.

Key words Raman spectroscopy · Wood preservatives · Boric acid · Japanese cedar · Aqueous solution

Introduction

During the last decade wood preservatives containing arsenic and heavy metals have been rapidly replaced because of environmental concerns. Boron compounds are often used for preservative treatment as they are less toxic to mammals while being regarded as both an effective insecticide and fungicide. However, boric acid and borax, the most common boron compounds, are readily eluted from wood by rainwater.

Boron compounds require stable fixation in wood and must have low toxicity in the environment. New processes of boron fixation have been proposed,[1–6] but the fixed compounds must still be effective as wood preservatives. To devise such a process of fixation, it is necessary to understand the physical and chemical behavior of boron species and the distribution of boron in wood before and after leaching. Accordingly, analysis of boron in timber plays an important role in the study of fixation mechanisms, whereas it is difficult to estimate boron in a solid state.

Raman spectroscopy is a useful, reliable technique for identifying boric acid and borates because of their characteristic Raman-active vibrations due to symmetry. This spectroscopy has been widely utilized to investigate boron species in various dispersed systems (e.g., solutions or glass) and is suitable for microscopic, nondestructive analysis.

There have been few reports on the Raman spectra of lignocellulosics, except those by Agarwal et al.[7,8] and Atalla and Agarwal,[9,10] until recently because the fluorescence arising from visible laser irradiation makes it difficult to obtain a spectrum by conventional Raman spectroscopy. Several Raman spectroscopic studies[11–14] on wood constituents have been reported, with a near-infrared laser being used as an excitation source. We have also reported on the identification of adhesives,[15–18] and detected boric acid as a preservative in wood[19] using Raman spectroscopy. In a preliminary study, we demonstrated that (1) the prominent Raman band at about $879\,cm^{-1}$ (ν_1) can be regarded as a reliable indicator of the BO_3 group and (2) most of the boron species are present as $B(OH)_3$ in Japanese cedar wood treated by impregnation with aqueous boric acid solutions.[19]

The aim of this study is to obtain more information on the behavior of boron species in treated wood through the use of Raman spectroscopy. In the present paper, we report changes in the intensity of the ν_1 band with increasing boric acid concentration in aqueous solution and the correlation between the intensity and the peak-top wavenumber. The

S. Yamauchi (✉) · S. Doi
Institute of Wood Technology, Akita Prefectural University, 11-1 Kaieisaka, Noshiro 016-0876, Japan
Tel. +81-185-52-6984; Fax +81-185-52-6976
e-mail: sigeru@iwt.akita-pu.ac.jp

Raman spectroscopic results are interpreted from the viewpoint of the chemical species around boron species. Moreover, the distributions of boron species in the treated wood are investigated on the basis of ν_1 band intensity.

Materials and methods

Wood samples

The wood blocks used as samples in this study were taken from an 80-year-old Japanese cedar and divided into two types by size. The A-type samples were $20(T) \times 20(R) \times 5(L)$ mm, and the B-type samples were $15(T) \times 15(R) \times 50(L)$ mm. Each block was kept at 25°C and 60% relative humidity (RH) in an environmental chamber to obtain a constant weight and then vacuum-impregnated with aqueous boric acid solutions. Boric acid was purchased from Wako Pure Chemical Industries and was used without further purification. The water used for preparing boric acid solutions was deionized by passage through an ion-exchange column and then distilled. All the A-type blocks were prepared from sapwood. Half of the B-type blocks were made from sapwood and half from heartwood.

Treatment with boric acid

Aqueous solutions for treatment ranged in boric acid concentration from 8.1×10^{-2} to 7.29×10^{-1} mol dm^{-3}. After overall immersion of wood blocks into an aqueous boric acid solution, the vessel holding the solution was placed in a vacuum desiccator. The internal pressure was evacuated with a water-jet pump until it became constant. The desiccator was closed and left to stand for an hour. The blocks were then removed out from the solution. The surplus solution on the surface of the block was quickly soaked up with filter paper, and the weight of the block taking up the boric acid solution was measured. After air-drying at $23° \pm 1°$C for 2 days, each block was kept in the chamber under the conditions noted above until a constant weight was obtained. Five A-type and two B-type replications were provided for an aqueous solution. A-type and B-type blocks treated by impregnation with pure water through the same procedures were adopted as control samples.

Raman spectroscopy

Fourier-transform (FT)-Raman spectra were recorded using a JEOL JIR7000W spectrometer equipped with an RS-RSU-200 Raman module and a TGS detector. The excitation source was an Nd^{3+}:YAG laser (1064.1 nm) in the 180° back-scattering configuration. The laser beam was focused onto the wood blocks to a point of about 0.5 mm diameter; the incident laser power was 220 mW, which is low enough to prevent irreversible thermal damage to the wood. To obtain good-quality spectra of wood samples, 1000–3000 scans were accumulated at about 2 cm^{-1} intervals (ca. 4 cm^{-1} spectral resolution). All the Raman spectra were recorded at ambient temperature. The wavenumber was calibrated using the 460 cm^{-1} line of carbon tetrachloride and the 1332 cm^{-1} line of diamond.

As for A-type blocks treated with boric acid, Raman spectra were measured only on the transverse face. The face to be irradiated by the laser was shaved to remove boric acid crystals from the surplus solution. Raman measurements were carried out with five A-type replications for each boric acid concentration. Two or more Raman spectra were recorded from each A-type block. When a point on a transverse face was measured, the same point on another transverse face was also measured. The treated B-type blocks were cut parallel to their radial face into two equal parts. Raman line maps on the new surfaces (radial face) were made in the longitudinal direction. The peak height of the Raman band at 879 cm^{-1} due to B(OH)$_3$ was determined in a spectrum from which the components of Japanese cedar wood were eliminated by a difference spectrum method.

Results and discussion

Figure 1 shows a comparison of the Raman spectra in the 400–2000 cm^{-1} region of boric acid in a solid state (microcrystals) with that dissolved in water at 7.29×10^{-1} mol dm^{-3}. A symmetrical BO$_3$ stretching vibration,[20] ν_1, which is Raman active and characteristic, appears at 879 cm^{-1} in the solid state. In the aqueous solution the same band is observed at a slightly lower wavenumber (875 cm^{-1}). Raman lines at 497 cm^{-1} (O—B—O bending, ν_2) and 1167 cm^{-1} (B—O—H bending, ν_3)[20] are apparent in the solid state but not detectable in the aqueous solution. The broad band at around 1620 cm^{-1} observed in the aqueous solution is assigned to a bending vibration of a H$_2$O
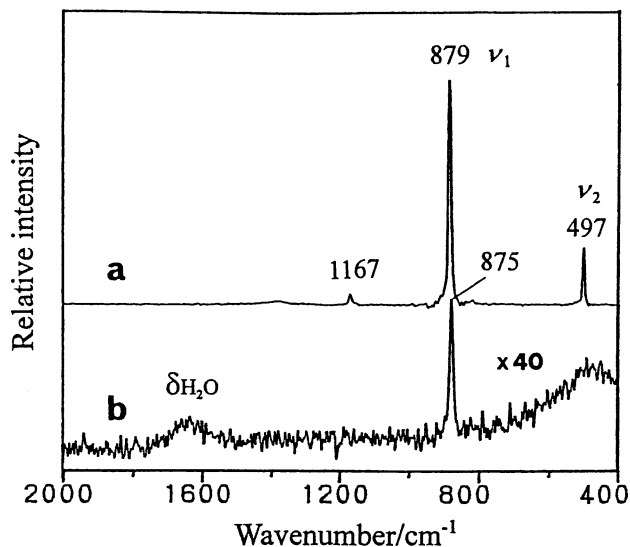

Fig. 1. Raman spectra of boric acid. *a*, microcrystals; *b*, aqueous solution at 7.29×10^{-1} mol dm^{-3}
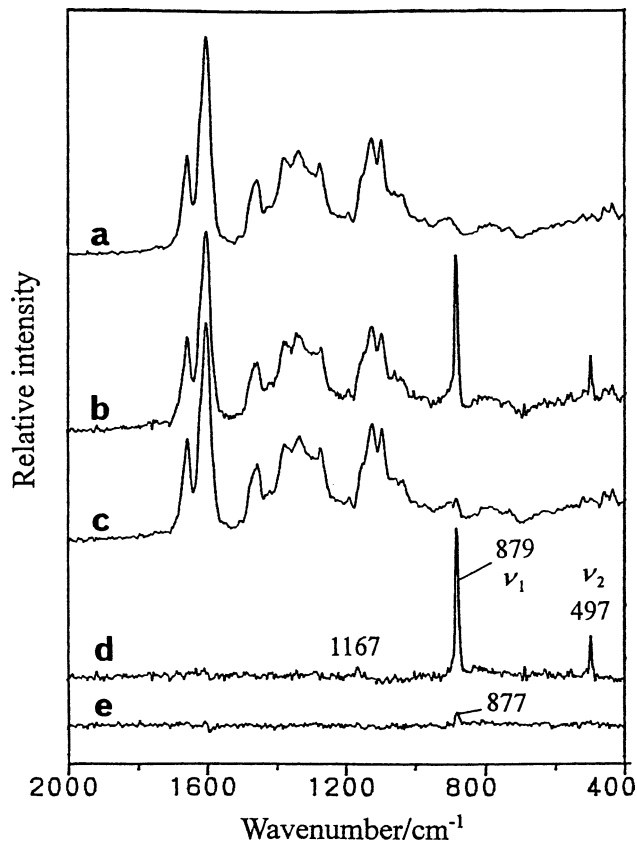
Fig. 2. Raman spectra of transverse faces (earlywood) of A-type blocks treated with aqueous solutions. *a*, A-type block treated with pure water; *b*, A-type block treated with $7.29 \times 10^{-1}\,\text{mol}\,\text{dm}^{-3}$ solution; *c*, A-type block treated with $2.43 \times 10^{-1}\,\text{mol}\,\text{dm}^{-3}$ solution; *d*, difference spectrum of *b* minus *a*; *e*, difference spectrum of *c* minus *a*

molecule. No boron species other than $B(OH)_3$ could be identified from the Raman spectra in the aqueous solutions used in this study.

Raman spectra of earlywood on a transverse face of A-type blocks treated with the aqueous solutions in the same wavenumber region are shown in Fig. 2. In general, Raman spectroscopy can be regarded as a surface analytical tool provided the sample is an opaque solid. An excitation light of 1064.1 nm scarcely penetrates the cell wall of the wood owing to its opacity. It can be presumed, therefore, that these spectra reflect only the compounds in an extremely short range from the transverse face.

The top Raman spectrum in Fig. 2 was obtained from a control wood block treated with pure water, and its spectral contour agrees fairly well with those of untreated Japanese cedar wood.[15,17] There was no significant difference in spectral contour between the earlywood and latewood of the control block, whereas the Raman band intensities of latewood were much larger than those of earlywood. In addition, the moisture content had little influence on the Raman spectra of the wood blocks after air-drying, as this spectroscopy is far less sensitive to water molecules than infrared spectroscopy.

Spectra *b* and *c* in Fig. 2 are representative Raman spectra of A-type blocks treated with boric acid solutions of 7.29

$\times 10^{-1}$ and $2.43 \times 10^{-1}\,\text{mol}\,\text{dm}^{-3}$, respectively. The intensities of Raman bands due to the BO_3 group varied considerably even in an A-type treated block. Spectrum *d* is expressed as $(b) - k \times (a)$, where *k* is a constant; that is, a difference spectrum removed the Raman bands due to wood components from spectrum *b*. Spectrum *e* was calculated from spectra *a* and *c* in the same way.

The ν_1 and ν_2 bands of the BO_3 group are obvious in spectrum *b*, and even the weakest band of ν_3 is detectable around $1167\,\text{cm}^{-1}$ in the difference spectrum *d*. For the wood block treated with the $2.43 \times 10^{-1}\,\text{mol}\,\text{dm}^{-3}$ solution, the ν_1 band of spectrum *e* is observable, but the wavenumber is slightly lower than that of spectrum *d*. Neither ν_2 nor ν_3 is discerned despite the use of the difference spectrum method.

No Raman band due to boron species, except ν_1, ν_2, and ν_3, could be detected in the $400–2000\,\text{cm}^{-1}$ region in any of the treated A-type wood blocks. Thus, it is suggested that $B(OH)_3$ is the dominant form of the boron species and the amount of $B(OH)_4^-$, polyborates, or other boron species in the treated wood blocks is much less than that of $B(OH)_3$. This is supported by previous Raman studies for borates in aqueous solution[21–24] and pH measurements for Japanese cedar.[25]

Correlation between ν_1 band intensity and boric acid concentration

The weights of A-type blocks at 25°C and 60% RH before treatment with aqueous boric acid solution were in the range of 0.577–0.882 g. As for the blocks impregnated fully with the solution, the weights were 2.30–2.49 g and were apparently independent of the boric acid concentration in aqueous solution. The weight gain (the mean of five replications) of the block after treatment is plotted versus the boric acid concentration in Fig. 3. An approximately linear relation is found between weight gain and the concentration. Based on the weight measurements, it is evident that all the lumens in the A-type block made from sapwood were readily impregnated with the aqueous solution and that little solution effused from the block during the air-drying and conditioning processes.

Figure 4 illustrates the plots of ν_1 band intensity normalized by the band peaking near $1600\,\text{cm}^{-1}$ due to the benzene ring versus the boric acid concentration. Peak height was adopted as band intensity. The bar corresponds to the region between the maximum and minimum band intensities at a given concentration. The normalization is of no worth unless the Raman spectra in Fig. 4 are recorded under the same conditions for Japanese cedar wood; hence the Raman measurements were made only on transverse faces of earlywood.

The plots exhibit two remarkable results. First, the ν_1 band intensity is far less linear with the boric acid concentration in an aqueous solution than the weight gain. Accordingly, the relation between the intensity and the weight gain is also nonlinear. Second, the minimum value hardly increases with the boric acid concentration despite a steep
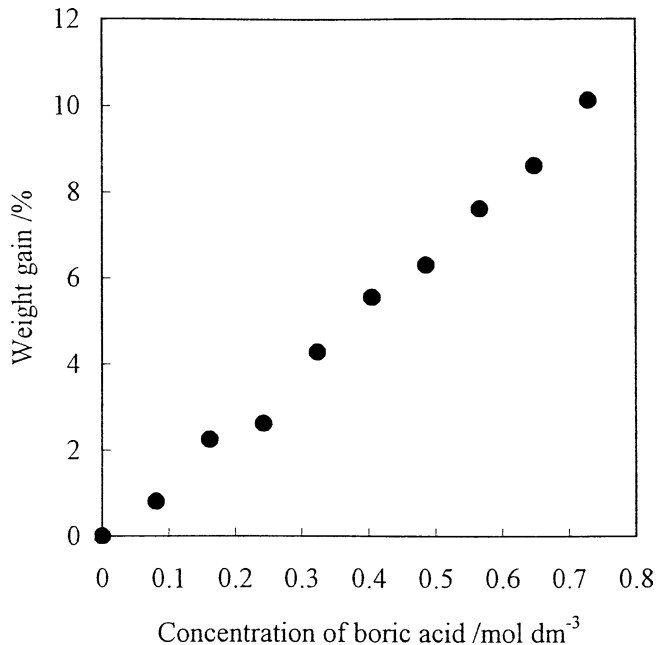
Fig. 3. Relation between the weight gain of the treated A-type block and the boric acid concentration of the aqueous solution used for treatment
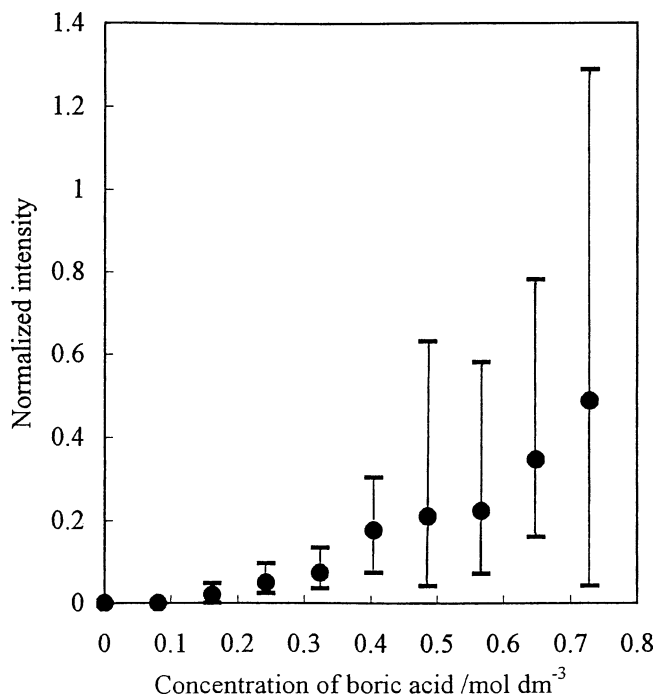

Fig. 4. Changes in ν_1 band intensity obtained by Raman measurements of transverse faces (earlywood) of treated A-type blocks with the boric acid concentration of the aqueous solution used for treatment. The bars indicate the maximum to minimum range for Raman measurements at a given concentration

increase in the maximum value. In the A-type wood samples treated with high-concentration solutions, large differences in the ν_1 band intensity were often observed between both transverse faces of a sample, whereas the

variation in intensity was not as large within a transverse face. The results suggest pronounced localization of boron in the longitudinal direction. The details are described later.

We first discuss the nonlinear relation. As seen in Fig. 4, the ν_1 band is not detected at a concentration of $8.1 \times 10^{-2}\,\mathrm{mol\,dm^{-3}}$, whereas a reasonable value for the weight gain is obtained. In other words, the result indicates a missing fraction of boron species in the Raman spectroscopic analysis. In addition, it appears that the ν_1 band intensity increases sharply at more than $3.24 \times 10^{-1}\,\mathrm{mol\,dm^{-3}}$, especially in maximum values; that is, there is a discontinuity in the range from 3.24×10^{-1} to $4.05 \times 10^{-1}\,\mathrm{mol\,dm^{-3}}$.

There are two possible explanations for the nonlinear relation. One is the complex formation of boron. It is generally accepted that chemical bonds are formed between $B(OH)_4^-$ and polyols containing diol groups in aqueous solution, and the coordination number of boron is four in the complexes.[26–29] The vibrational modes of B—O bonds in the complexes should be entirely different from those in $B(OH)_3$, and their Raman intensities may be extremely weak. Therefore, it can be seen that the boron complexes with wood constituent molecules correspond to the missing fraction. However, the results reported in this study provide no experimental evidence for the formation of boron complexes in the treated wood block. The complexes presumably, even though complexation occurs, present only in small amounts in the treated wood blocks.

The second explanation is the penetration of $B(OH)_3$ into the cell wall. Based on the mechanism of swelling of wood in liquid,[30,31] the penetration phenomenon for $B(OH)_3$ can be described as follows. The aqueous boric acid solution passes rapidly from lumen to lumen through bordered pits and fills almost all of the lumens in A-type wood blocks by pressure reduction. At the same time or immediately afterward, water molecules begin to penetrate the cell wall together with dissolved $B(OH)_3$. Forming hydrogen bonds with the OH groups of the wood components, the water molecules and $B(OH)_3$ penetrate more deeply into the cell wall.

During the subsequent air-drying process, the concentration of aqueous boric acid solution in the lumen increases gradually when water molecules evaporate from the wood block. From the viewpoint of chemical equilibrium, $B(OH)_3$ in aqueous solution moves into the cell wall by concentration. It can be presumed that all of the $B(OH)_3$ enters the cell wall provided the initial boric acid concentration of the aqueous solution is adequately low, because almost all of the water molecules exist in the cell wall and no free water remains in the lumens after air-drying. There is, however, an upper limit to the amount of $B(OH)_3$ that can be contained in the cell wall, and therefore excess $B(OH)_3$ precipitates as microcrystals when the solution in the lumen or intercellular space reaches a saturation point. The microcrystals probably adhere to the surface of the cell wall, and the amount increases as the drying process proceeds.

Briefly, after the air-drying process, $B(OH)_3$ exists only in the cell walls of wood blocks treated with adequately low-concentration solutions. When the initial boric acid concentration is beyond a certain value, boric acid microcrystals

separate out in the lumen. An EPMA study by Furuno et al.[32] has supported the existence of boron in the cell walls of Japanese cedar treated with aqueous boric acid solution.

It is evident that the number of $B(OH)_3$ units per unit volume in the microcrystalline state greatly exceeds that in the treated cell wall, even if the wall is saturated with $B(OH)_3$. Therefore, it is expected that the ν_1 band intensity obtained from boric acid microcrystals is much stronger than that from the cell wall containing $B(OH)_3$ under the same conditions of laser irradiation, although an effective determinant for the ν_1 band intensity is not the amount of $B(OH)_3$ alone. Consequently, the results in Fig. 4 suggest that boric acid precipitates as microcrystals in the vicinity of either of the transverse faces of the A-type wood blocks on treatment with a $4.05 \times 10^{-1}\,mol\,dm^{-3}$ or more concentrated boric acid solution.

Peak-top wavenumber of ν_1 band

The plots of the normalized ν_1 band intensity against peak-top wavenumbers are shown in Fig. 5. Although every peak-top of the ν_1 band is detected in the short range of $871–879\,cm^{-1}$, there is a tendency for the peak-top to have higher wavenumbers with increasing ν_1 band intensity. It is worth noting that all the peak-top positions are located at the upper limit of $879\,cm^{-1}$, which is equal to the value for the microcrystals shown in Fig. 1, in the intensity region above 0.3. This indicates that most of the $B(OH)_3$ exists as microcrystals at the spot where a strong ν_1 band appears, which supports our proposal for the behavior of $B(OH)_3$ during the air-drying process.
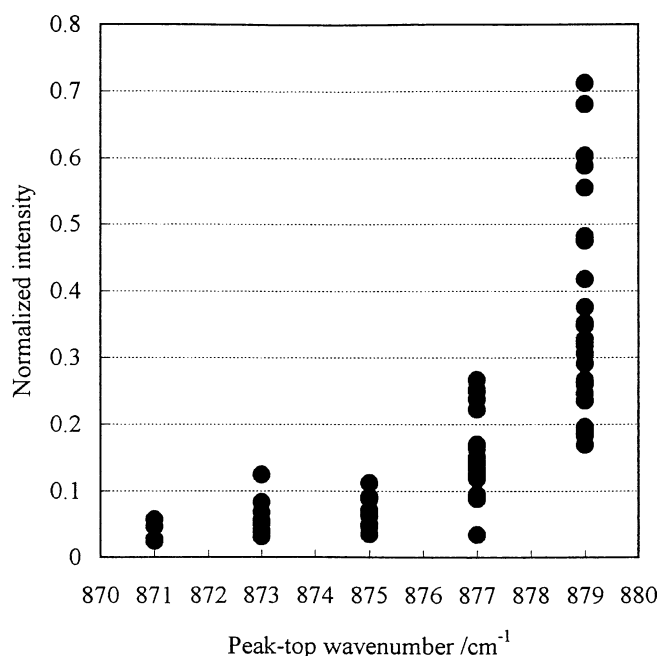
In contrast, the peak-top wavenumber varies from 871 to $879\,cm^{-1}$ in the low-intensity (< 0.3) region. In particular, most values are $875\,cm^{-1}$ or less in the region below 0.1. The change of chemical species around the $B(OH)_3$ unit better explains the variations of the peak-top wavenumber in the small range than the chemical bonds of boron (e.g., the formation of complexes) because the wavenumbers of B—O vibrations in the complexes should be entirely different from those in $B(OH)_3$.

The $B(OH)_3$ unit in the treated wood can be classified into two groups according to the chemical species of the nearest neighbor. One is a group having only the same units around itself, such as microcrystals. The other group consists of $B(OH)_3$ units penetrating the cell wall; hence, possible chemical species next to the $B(OH)_3$ unit are the constituents of wood, such as cellulose, hemicellulose, lignin, and water molecules in addition to the same unit.

The results shown in Fig. 5 suggest that $B(OH)_3$ at irradiation sites, if only the weak ν_1 bands are obtained, does not exist as microcrystals. It is expected that the $B(OH)_3$ unit in the cell wall forms hydrogen bonds with the bound water molecules or wood constituents in the nearest neighbor sphere, although it is not clear why the ν_1 band shifts to a wavenumber lower than that of the microcrystals.

Comparison of latewood with earlywood

The differences between the Raman spectra of both earlywood and latewood on a transverse face of the treated A-type block are described here. The Raman measurements alternating between earlywood and latewood were carried out as shown in Fig. 6a. The Raman spectral changes on the
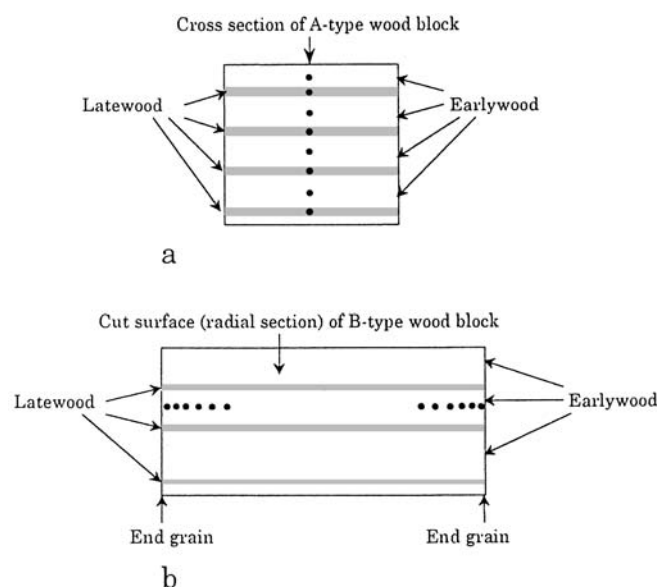

Fig. 5. Plots of ν_1 band intensity against the peak-top wavenumber in Raman measurements of a transverse face (earlywood) of a treated A-type block

Fig. 6. Measurement points on the surface of wood blocks. **a** Points on a transverse face of an A-type block corresponding to that in Fig. 7. **b** Points on the newly cut surface (radial face) of a B-type block corresponding to that in Fig. 9. *Filled circles*, laser irradiation spot with a diameter of about 0.5 mm
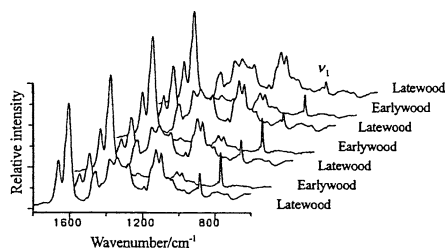
Fig. 7. Raman spectral changes between earlywood and latewood on a transverse face of an A-type block treated with an aqueous boric acid solution at $6.48 \times 10^{-1}\,mol\,dm^{-3}$
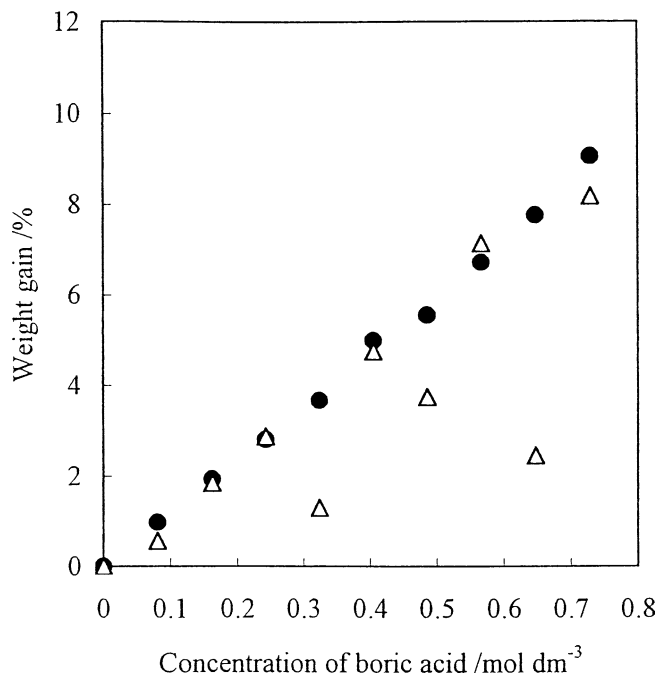

Fig. 8. Plots of the weight gains of treated B-type blocks versus the boric acid concentration used of the aqueous solution used for treatment. *Circles*, sapwood, *triangles*, heartwood

transverse face of the wood blocks treated with $6.48 \times 10^{-1}\,mol\,dm^{-3}$ solutions are depicted in Fig. 7. The Raman band intensities attributed to the wood constituents in the latewood are 1.5–2.0 times those in earlywood, although there is no significant difference in the line shape of the Raman bands between them. It is likely that the variation in the intensity of the Raman band due to wood corresponds to that of the apparent specific gravity of the wood portion at the laser spot. Interestingly, it is apparent from Fig. 7 that the intensities of the ν_1 band observed for earlywood are larger than those for latewood.

In the blocks treated with low-concentration solutions ($< 2.43 \times 10^{-1}\,mol\,dm^{-3}$), a reverse correlation was occasionally obtained; that is, there was an increase in the Raman band intensity of ν_1 with the apparent specific gravity at the laser spot, which was not as appreciable owing to the low intensity of the ν_1 band. Moreover, such a correlation was also observed in the Raman measurements of blocks treated with high-concentration solutions when the ν_1 intensity was sufficiently weak. As a result, the factor that determines whether the intensity of ν_1 increases or decreases with those of the Raman bands due to the wood constituents would not be the initial concentration of the boric acid solution for the treatment but the amount of $B(OH)_3$ on or near the transverse face of the treated wood block.

A likely explanation for the noteworthy results is based on our proposal for the behavior of $B(OH)_3$. The amount of $B(OH)_3$ contained in the cell wall per unit volume of a wood block is much larger in the latewood portion than in the earlywood portion because the cell wall/lumen volume ratio of latewood is larger than that of earlywood. Conversely, less $B(OH)_3$ precipitate is deposited in the lumens of latewood than in those of earlywood after air-drying. Accordingly, it is anticipated that a stronger ν_1 band intensity would be observed in earlywood than in latewood if precipitation of $B(OH)_3$ occurs. In the absence of a precipitate, the changes in intensity of the ν_1 band are not necessary, in accordance with the results in Fig. 7.

Distribution of $B(OH)_3$ in the longitudinal direction

We have discussed only $B(OH)_3$ on or near the transverse face of wood samples. Hence, the inner $B(OH)_3$ is now investigated. The A-type blocks were not long enough to

study the inner distribution of $B(OH)_3$ in wood, so we adopted B-type blocks, in which the longitudinal length was 50 mm.

Figure 8 shows the weight gain versus the initial concentration of boric acid of sapwood and heartwood in B-type blocks. In the blocks from sapwood, the gain increases smoothly with increasing concentration, as in the A-type blocks. The increase shows complete impregnation with boric acid solution in each sample. In contrast, such a continuous increase is not observed in the heartwood blocks, and there are several distinct discontinuities in the variation of weight gain with the concentration of boric acid. Thus, it is not easy to impregnate entirely the B-type blocks comprised of heartwood with boric acid solution even through a vacuum process. This is ascribed to the much larger portion of closed or enclosed (or both) bordered pits compared to that in earlywood.

The Raman measurements were performed in the longitudinal direction in earlywood of a cut surface (radial face) of B-type blocks treated with $7.29 \times 10^{-1}\,mol\,dm^{-3}$ solution. Two Raman line maps are illustrated in Fig. 9 (cf. Fig. 6b). These maps show representative spectral changes for sapwood and heartwood. All the spectra are given as a difference spectrum by subtracting the components due to wood constituents from the raw spectrum. Although ν_1 appears as a strong band at the measurement points in the neighborhood of the cut ends, the intensity decreases sharply with increasing distance from the cut end. The ν_1 band is undetectable outside of an extremely limited range of depth from the cut end, especially for the sapwood block. The same spectral changes were observed near the opposite cut end.
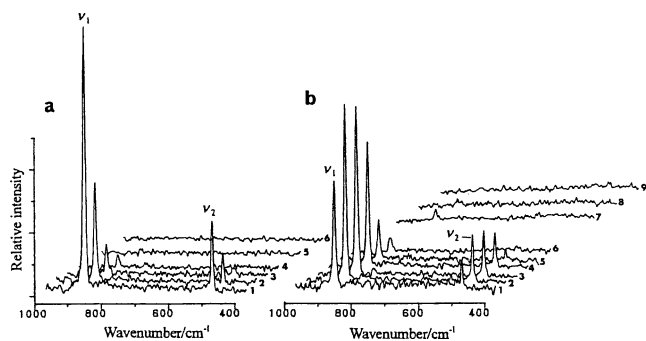
Fig. 9. Line maps of various Raman spectra in the longitudinal direction of treated B-type blocks. **a** Sapwood – distance from end grain: *1*, 0.5 mm; *2*, 1.0 mm; *3*, 1.5 mm; *4*, 2.0 mm; *5*, 3.0 mm; *6*, 4.0 mm. **b** Heartwood – *1*, 0.5 mm; *2*, 1.0 mm; *3*, 1.5 mm; *4*, 2.0 mm; *5*, 2.5 mm; *6*, 3.0 mm; *7*, 5.0 mm; *8*, 6.0 mm; *9*, 7.0 mm

These results, which suggest that $B(OH)_3$ microcrystalline precipitates only in the vicinity of the cut end, are notable, although Raman measurements have not been carried out over the entire cut surfaces. A complete explanation for such a localization of the boric acid microcrystals has not been provided; however, the drying process and the cell structure of wood samples are likely to be factors affecting their distribution. Further investigation requires a more detailed two-dimensional analysis.

Conclusions

We explored the distribution of boron species in Japanese cedar treated with aqueous boric acid solutions by Raman spectroscopy. The results revealed that $B(OH)_3$ is the dominant form in the boron species and localization of $B(OH)_3$ microcrystals occurs during the air-drying process; the results have been interpreted in terms of the physical and chemical behavior of $B(OH)_3$ species in wood. Based on the intensity and peak-top wavenumber of the Raman band (ν_1) due to $B(OH)_3$, it is proposed that the $B(OH)_3$ unit in wood can be classified into two groups based on the chemical species around it. One group comprise the microcrystalline state of $B(OH)_3$ precipitated in lumens, and the other comprises the $B(OH)_3$ units penetrating the cell wall. An obvious tendency recognized from Raman line maps in the longitudinal direction is that $B(OH)_3$ microcrystals are made significantly more abundant near cut ends in a long-axial wood block (e.g., the B-type block) via the air-drying process.

References

1. Murphy RJ, Barnes HM, Gray SM (1995) Decay and soil depletion studies with polymer/boron preservative systems. For Prod J 45: 77–81
2. Pizzi A, Baecker A (1996) A new boron fixation mechanism for environment friendly wood preservatives. Holzforschung 50:507–510
3. Thevenon MF, Pizzi A, Haluk JP (1997) Non toxic albumin and soja protein borates as ground-contact wood preservatives. Holz Roh Werkstoff 55:293–296
4. Thevenon MF, Pizzi A, Haluk JP (1998) Protein borates as non-toxic, long-term, wide-spectrum, ground-contact wood preservatives. Holzforschung 52:241–248
5. Yalinkilic MK, Imamura Y, Takahashi M, Yalinkilic AC (1999) In situ polymerization of vinyl monomers during compressive deformation of wood treated with boric acid to decay boron leaching. For Prod J 49:43–51
6. Toussaint-Dauvergne E, Soulounganga P, Gérardin P, Loubinoux B (2000) Glycerol/glyoxal: a new boron fixation system for wood preservation and dimensional stabilization. Holzforschung 54:123–126
7. Agarwal UP, Atalla RH (1986) In-situ Raman microprobe studies of plant cell walls: macromolecular organization and compositional variability in the secondary wall of *Picea mariana* (mill.) B.S.P. Planta 169:325–332
8. Agarwal UP, Atalla RH, Forsskåhl I (1995) Sequential treatment of mechanical and chemimechanical pulps with light and heat: a Raman spectroscopic study. Holzforschung 49:300–312
9. Atalla RH, Agarwal UP (1984) Raman microprobe evidence for lignin orientation in the cell walls of native woody tissue. Science 227:636–638
10. Atalla RH, Agarwal UP (1986) Recording Raman spectra from plant cell wall. J Raman Spectrosc 17:229–231
11. Takei T, Iijima T, Higaki M, Fukuzumi T (1994) The properties and chemical components of mangroves. V. Lignin carbohydrate complexes from *Bruguiera gymnorrhiza* wood (in Japanese). Mokuzai Gakkaishi 40:868–873
12. Takei T, Kato N, Iijima T, Higaki M (1995) Raman spectroscopic analysis of wood and bamboo lignin (in Japanese). Mokuzai Gakkaishi 41:229–236
13. Ona T, Sonoda T, Ito K, Shibata M, Kato T, Ootake Y (1998) Nondestructive determination of hemicellulosic neutral sugar composition in native wood by Fourier transfer Raman spectroscopy. J Wood Chem Technol 18:27–41
14. Agarwal UP, Ralph SA (1997) FT-Raman spectroscopy of wood: identifying contributions of lignin and carbohydrate polymers in the spectrum of black spruce (*Picea mariana*). Appl Spectrosc 51:1648–1655
15. Yamauchi S, Koizumi A, Kurimoto Y, Tamura Y (1996) Vibrational spectroscopic studies on wood and wood-based materials. I. Detection of MDI in wood by measurement of Raman effect (in Japanese). J Adhes Soc Jpn 32:453–456
16. Yamauchi S, Koizumi A, Kurimoto Y, Tamura Y (1997) Vibrational spectroscopic studies on wood and wood-based materials. II. Infrared and Raman spectroscopic investigation for MDI penetration behavior in wood (in Japanese). J Adhes Soc Jpn 33:95–102
17. Yamauchi S, Tamura Y, Kurimoto Y, Koizumi A (1997) Vibrational spectroscopic studies on wood and wood-based materials. III. Identification of adhesives in wood by using FT-Raman spectroscopy as a nondestructive analytical method (in Japanese). J Adhes Soc Jpn 33:380–387
18. Yamauchi S, Tamura Y, Kurimoto Y, Koizumi A (1999) Vibrational spectroscopic studies on wood and wood-based materials. IV. Solvent effects of diluent on MDI penetration behavior in wood (in Japanese). J Adhes Soc Jpn 35:300–308
19. Yamauchi S, Doi S (2000) A Raman spectroscopic study for boric acid in wood: sugi wood treated with aqueous boric acid solutions (in Japanese). Wood Preserv 26:266–272
20. Servoss RR, Clark HM (1957) Vibrational spectra of normal and isotopically labelled boric acid. J Chem Phys 26:1175–1178
21. Maya L (1976) Identification of polyborates and fluoroborate ions in solution by Raman spectroscopy. Inorg Chem 15:2179–2184
22. Maeda M, Hirao T, Kotaka M, Kakihana H (1979) Raman spectra of polyborates ions in aqueous solution. J Inorg Nucl Chem 41:1217–1220
23. Adams CJ, Clark IE (1983) On the nature of the peroxoborate ion in solution. Polyhedron 2:673–675
24. Flanagan J, Griffith WP, Powell RD, West AP (1989) Nature of peroxoborate species in aqueous solution: a study by boron-11 nuclear magnetic resonance and Raman spectroscopy. J Chem Soc Dalton Trans 1651–1655

25. Takenami K (1964) Studies on the discoloration of wood. I. Sensitivities of various wood species for the dyeing effect with iron. Mokuzai Gakkaishi 10:22–29
26. Deuel H, Neukom H, Weber F (1948) Reaction of boric acid with polysaccharides. Nature 161:96–97
27. Böeseken J (1949) The use of boric acid for the determination of the configuration of carbohydrates. Adv Carbohydr Chem 4:189–210
28. Henderson WG, How MJ, Kennedy GR, Mooney EF (1973) The interconversion of aqueous boron species and the interaction of borate with diols: a ^{11}B NMR study. Carbohydr Res 28:1–12
29. Gey C, Noble O, Perez S, Taravel FR (1988) Complexes of borate ions with guar D-galacto-D-mannan polymer and related model compounds. Carbohydr Res 173:175–184
30. Nayer AN, Hossfeld RL (1949) Hydrogen bonding and the swelling of wood in various organic liquids. J Am Chem Soc 71:2852–2855
31. Ishimaru Y, Sakai H (1988) Swelling of wood in liquid mixtures. I. Water-ethanol and water-acetone (in Japanese). Mokuzai Gakkaishi 34:889–895
32. Furuno T, Goto T, Katoh S (2001) EPMA observation of wood-mineral composites using the silicate-boron compound system and estimation of fire resistance by oxygen index method (in Japanese). J Soc Mater Sci Jpn 50:383–390